arXiv:nucl-th/0505007v4 17 Feb 2006

Determination of S_{17} from ^{8}B breakup by means of the method of continuum-discretized coupled-channels

K. Ogata,[1,*] S. Hashimoto,[1] Y. Iseri,[2] M. Kamimura,[1] and M. Yahiro[1]

[1]*Department of Physics, Kyushu University, Fukuoka 812-8581, Japan*
[2]*Department of Physics, Chiba-Keizai College, Todoroki-cho 4-3-30, Inage, Chiba 263-0021, Japan*

(Dated: February 9, 2008)

The astrophysical factor for ^{7}Be$(p,\gamma)^8$B at zero energy, $S_{17}(0)$, is determined from an analysis of ^{208}Pb(^{8}B, p+^{7}Be)^{208}Pb at 52 MeV/nucleon by means of the method of continuum-discretized coupled-channels (CDCC) taking account of all nuclear and Coulomb breakup processes. The asymptotic normalization coefficient (ANC) method is used to extract $S_{17}(0)$ from the calculated breakup cross section. The main result of the present paper is $S_{17}(0) = 20.9^{+2.0}_{-1.9}$ eV b. The error consists of 8.4% experimental systematic error and the error due to the ambiguity in the s-wave p-^{7}Be scattering length. This value of $S_{17}(0)$ differs from the one extracted with the first-order perturbation theory including Coulomb breakup by dipole transitions: 18.9 ± 1.8 eV b. It turns out that the difference is due to the inclusion of the nuclear and Coulomb-quadrupole transitions and multi-step processes of all-order in the present work. The p-^{7}Be interaction potential used in the CDCC calculation is also used in the ANC analysis of ^{7}Be$(p,\gamma)^8$B. The value of $S_{17}(0) = 21.7^{+0.62}_{-0.55}$ eV b obtained is consistent with the previous one obtained from a precise measurement of the p-capture reaction cross section extrapolated to zero incident energy, $S_{17}(0) = 22.1 \pm 0.6$ (expt) ± 0.6 (theo) eV b, where (theo) stands for the error in the extrapolation. Thus, the agreement between the values of $S_{17}(0)$ obtained from direct ^{7}Be$(p,\gamma)^8$B and indirect ^{8}B-breakup measurements is significantly improved.

PACS numbers: 24.10.Eq, 25.60.Gc, 25.70.De, 26.65.+t

I. INTRODUCTION

The solar neutrino problem is one of the central issues in the neutrino physics [1]. The current interpretation of the solar-neutrino deficit is the neutrino oscillation induced by the mass difference among ν_e, ν_μ, and ν_τ, and their mixing angles [2]. Attention is now focused on the determination of the oscillation parameters. The cross section of the p-capture reaction ^{7}Be$(p,\gamma)^8$B at incident energy in the center-of-mass (c.m.) frame of the p-^{7}Be system $E_{\rm c.m.} \sim 0$ plays an essential role in the solar-neutrino phenomenology, since the observed flux of ^{8}B neutrino is proportional to it; the magnitude of the cross section $\sigma_{p\gamma}(E_{\rm c.m.})$ is customarily expressed by the astrophysical factor $S_{17}(E_{\rm c.m.}) \equiv \sigma_{p\gamma}(E_{\rm c.m.})E_{\rm c.m.}\exp[2\pi\eta]$, where η is the Sommerfeld parameter. The required accuracy of $S_{17}(0)$, to determine the neutrino oscillation parameters with sufficient accuracy, is the error within 5% [3].

Recently, precise measurement of $\sigma_{p\gamma}(E_{\rm c.m.})$ was carried out by Junghans *et al.* [4] at energies of $E_{\rm c.m.}$ =116–2460 keV, which are low but still higher than stellar energies (~ 20 keV). Extrapolating the measured $S_{17}(E_{\rm c.m.})$ to $E_{\rm c.m.} = 0$ using a three-cluster model [5] for ^{8}B structure, they derived $S_{17}(0) = 22.1 \pm 0.6$ (expt) ± 0.6 (theo) eV b. The three-body model, however, did not simultaneously reproduce the magnitude and the energy-dependence of $S_{17}(E_{\rm c.m.})$ sufficiently well. Moreover, as pointed out in Ref. [6], the uncertainty of the s-wave p-^{7}Be scattering length (with about 50% error) prevents one from determining $S_{17}(0)$ with very high accuracy.

Because of the difficulty of the direct measurement of $\sigma_{p\gamma}(E_{\rm c.m.})$ at stellar energies, alternative indirect measurements were proposed. Coulomb dissociation [7, 8, 9, 10, 11, 12, 13] of ^{8}B is one of such indirect measurements. So far, extraction of $S_{17}(0)$ from these experiments has been based on the virtual photon theory with the assumption of ^{8}B dissociation by virtual electric dipole (E1) photon absorption. Nuclear interaction and absorption of quadrupole (E2)- and multi-photons were not taken into account. The value thus extracted from the RIKEN experiment at 52 MeV/nucleon was $S_{17}(0) = 18.9 \pm 1.8$ eV b [9]. In the analysis of the MSU experiment [12, 13] measured at 44 and 83 MeV/nucleon, the E2 contribution to one-step process was estimated from the parallel-momentum-distribution of ^{7}Be fragment and subtracted from the breakup spectrum of ^{8}B. As a result, the extracted $S_{17}(0)$ was $17.8^{+1.4}_{-1.2}$ eV b, which is smaller than the value obtained at RIKEN mentioned above. However, the analysis of the angular distribution of the ^{8}B breakup cross section of the RIKEN experiment showed no contribution of E2 transitions. Moreover, the recent experiment at rather high energy, 250 MeV/nucleon, done at GSI [11] showed that the E2 contribution was negligibly small; the resulting $S_{17}(0)$ was $18.6 \pm 1.2 \pm 1.0$ eV b. Even though the significance of E2 transitions can be energy-dependent, the conclusions from the MSU and RIKEN measurements at similar energies look inconsistent and roles of the E2 component are still not clear. More seriously, there exists a non-negligible discrepancy of about 15% between the values of $S_{17}(0)$ mentioned above that are derived from direct p-capture and indirect ^{8}B-breakup measurements.

Very recently, it was shown by a semiclassical calculation of ^{208}Pb(^{8}B, p+^{7}Be)^{208}Pb at 52 MeV/nucleon that the discrepancy mentioned above was significantly reduced by taking account of nuclear-breakup components, E2, and higher-order Coulomb breakup processes [14]. Motivated by this re-

---

[*] Electronic address: kazu2scp@mbox.nc.kyushu-u.ac.jp

sult, we attempt in the present paper to extract a reliable value of $S_{17}(0)$ analyzing the ^{8}B dissociation experiment measured at RIKEN [7, 8, 9], with the method of continuum-discretized coupled-channels [15, 16] (CDCC), assuming a p+^{7}Be+A three-body model of the system, where A stands for the target nucleus. The result of the analysis is then used to extract $S_{17}(0)$ by means of the asymptotic normalization coefficient (ANC) method [17]. CDCC has been successful in describing various processes in which effects of projectile-breakup are essential [18, 19, 20, 21, 22, 23, 24, 25, 26]. It has been successfully applied also to ^{8}B nuclear and Coulomb breakup processes [13, 27, 28, 29]. In the CDCC calculation of the present work, we include all nuclear and Coulomb breakup processes, and take account of the intrinsic spins of both p and ^{7}Be using the channel spin representation and the consistency of the p-^{7}Be interaction potential used in the CDCC calculation with the s-wave p-^{7}Be scattering length. The wave function of ^{8}B used in the CDCC calculation is found to be consistent with the measured cross section of ^{7}Be(p,γ)^{8}B at low energies. We then use the calculated breakup cross section and the p-^{7}Be separation energy in the ^{8}B nucleus to obtain $S_{17}(0)$ by the ANC method. An important advantage of the ANC method is that there is no restriction of the reaction mechanisms. In addition, the uncertainty of $S_{17}(0)$ due to the use of the ANC method can quantitatively be evaluated [26, 29].

The construction of the present paper is as follows. First, we describe how to extract the ANC from the three-body model CDCC analysis of ^{8}B breakup. We show that under a condition, which is satisfied in the present analysis, the calculated cross section is proportional to the square of the ANC for the ground state of ^{8}B. This is by no means trivial since the CDCC wave function contains not only the ground state of ^{8}B but also its continuum states. We describe in the later section the condition and the angular region of ^{8}B breakup in which it is satisfied. Second, we determine $S_{17}(0)$ from ^{208}Pb(^{8}B, p+^{7}Be)^{208}Pb at 52 MeV/nucleon by the ANC method, taking account of all order nuclear and Coulomb breakup processes. It should be noted that in our CDCC calculation interference between nuclear- and Coulomb-breakup amplitudes is explicitly included. We make use of the eikonal-CDCC method [30] (E-CDCC), with some modifications, to obtain the scattering amplitudes corresponding to large values of the orbital-angular-momentum L of relative motion between the projectile and the target nucleus. We then construct a hybrid amplitude from the results of E-CDCC and CDCC. This makes it possible to carry out very accurate analyses with high computational speed [30]. Uncertainties of the extracted $S_{17}(0)$ are carefully evaluated. Finally, we discuss the contributions of nuclear breakup, E2 transitions, and higher-order processes on the extracted value of $S_{17}(0)$. The ANC method is also applied to direct ^{7}Be(p,γ)^{8}B measurement assuming the same p-^{7}Be potential in the calculation of the direct capture process as used in the CDCC analysis. We show the difference between the values of $S_{17}(0)$ derived from direct and indirect measurements is essentially removed by the present analysis.

In Sec. II A we describe how to extract the ANC from the CDCC analysis of ^{8}B breakup. Formulation of modified E-CDCC and construction of the hybrid scattering amplitude are described in Sec. II B. We analyze in Sec. III B the ^{8}B breakup cross section measured at RIKEN with CDCC and extract $S_{17}(0)$ by the ANC method. Uncertainties of the extracted $S_{17}(0)$ are quantitatively evaluated in Sec. III C. In Sec. III D, the value of the extracted $S_{17}(0)$ is compared with the result of the virtual photon theory and the roles of nuclear breakup, E2 transitions, and higher-order processes are discussed. We discuss in Sec. III E the application of the ANC method to precise direct measurement of ^{7}Be(p,γ)^{8}B that confirms the consistency of its result with the ^{8}B breakup analysis. Finally summary and conclusions are given in Sec. IV.

II. FORMULATION

A. Extraction of ANC from ^{8}B breakup

In this subsection we describe our method of extracting $S_{17}(0)$ by p+^{7}Be+A three-body model CDCC analysis of elastic ^{8}B breakup reaction combined with the ANC method [17]. We recapitulate the ANC method below, partly to introduce notations. At very low incident energies, the p-capture reaction ^{7}Be(p,γ)^{8}B leading to the ground state of ^{8}B is extremely peripheral because of the Coulomb barrier. The T-matrix element of the reaction, therefore, depends on the overlap between the ground state wave functions of ^{7}Be and ^{8}B only in the tail region, where the radial part of the overlap has the following form

$$\begin{aligned} \varphi_{\rm r}^{(0)}(r) &\equiv \langle \phi_7^{(0)}(\xi_7)|\phi_8^{(0)}(\xi_7,\mathbf{r})\rangle_{\xi_7,\hat{\mathbf{r}}} \\ &\sim CW_{-\eta,\ell_0+1/2}(2k_0 r)/r, \quad r > R_{\rm N}, \end{aligned} \tag{1}$$

where $R_{\rm N}$ is the range of the nuclear interaction between p and ^{7}Be of about 4 fm, $\phi_7^{(0)}$ ($\phi_8^{(0)}$) is the ground state wave function of ^{7}Be (^{8}B), k_0 is the relative momentum in the unit of $\hbar$ between p and ^{7}Be, ξ_7 stands for the internal coordinates of the seven-nucleon system, and $W_{-\eta,\ell_0+1/2}$ is the Whittaker function where ℓ_0 is the orbital angular momentum of the p-^{7}Be relative motion in the ground state of ^{8}B; $\ell_0 = 1$ in the present case. The constant C in Eq. (1) is the ANC of our interest. The cross section $\sigma_{p\gamma}(0)$, and consequently $S_{17}(0)$, are proportional to C^2. Thus, one can evaluate them once the ANC, C, is known. The cross section of any reaction in which a proton is transferred to or from ^{8}B is proportional to C^2 in DWBA if the reaction is peripheral in the sense that it takes place when the transferred proton is distant from ^{7}Be more than the range $R_{\rm N}$. Based on this idea, DWBA analyses of proton transfer reactions such as ^{10}Be(^{7}Be,^{8}B)^{9}Be [31] and ^{14}N(^{7}Be,^{8}B)^{13}C [32] have successfully been made to obtain the required ANC.

In the present paper we analyze the data of ^{8}B elastic breakup in which the fragments ^{7}Be and p are ejected into very forward angles. For brevity, we henceforth call such a process breakup into forward angles. Since the breakup in such a case takes place at large distance R of ^{8}B from the target nucleus, it is mostly due to Coulomb interaction. The operator of the interaction is proportional to r^n with $n \geq 1$.

Therefore, the dominant contribution to the T matrix is from the region of r larger than the range of nuclear interaction $R_{\rm N}$ between the fragments. This is numerically confirmed as described in Sec. III C. The reaction, therefore, is peripheral in the sense described above. Thus, the ANC can be obtained if its cross section is reproduced and is shown to be proportional to C^2 by theory. We show in the following that the cross section is well reproduced by CDCC and is in good approximation proportional to C^2 in the present case.

We describe ^{8}B breakup at 52 MeV/nucleon with the p+^{7}Be+A three-body model illustrated in Fig. 1. Let us assume for simplicity that A is infinitely heavy. The triple differential cross section for (^{8}B,^{7}Be+p) reaction is given by $\mathcal{D}\rho|\mathfrak{T}|^2$ with a given constant $\mathcal{D}$ and the three-body phase space factor ρ [33]. The T-matrix element of ^{8}B breakup is

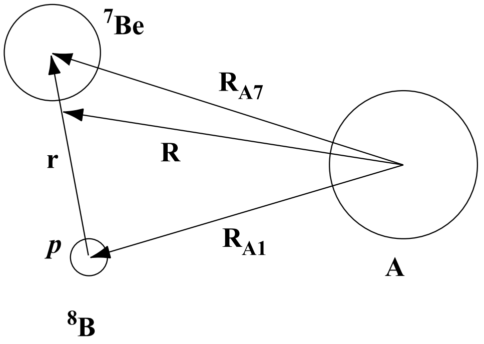

FIG. 1: Illustration of the p+^{7}Be+A three-body system, where A is a target.

$$\mathfrak{T}=\langle\chi_1\chi_7\phi_7^{(0)}|V|\Psi\rangle, \tag{2}$$

with

$$V=v_{\rm A7}(\mathbf{R}_{\rm A7},\xi_7)+U_{\rm A1}(\mathbf{R}_{\rm A1})+v_{17}(\mathbf{r},\xi_7),$$

where $v_{\rm XY}$ ($U_{\rm XY}$) is the interaction (distorting potential) between two nuclei X and Y, where the subscripts 1, 7, and A stand for p, ^{7}Be, and A, respectively. The function χ_1 (χ_7) is the plane wave of relative motion between A and the outgoing p (^{7}Be), and Ψ is the exact wave function of the system with the incident plane wave of relative motion between ^{8}B and A in the initial channel.

In the RIKEN experiment that we analyze in the present work, emitted fragments were measured at forward angles with the ^{7}Be in the ground state [7, 8, 9]. We assume that ^{7}Be stays in its ground state in the course of ^{8}B breakup. We have confirmed the validity of this assumption by a ^{3}He+^{4}He+^{208}Pb three-body model CDCC calculation of the scattering of ^{7}Be on ^{208}Pb at 52 MeV/nucleon. The cross sections of non-elastic processes including breakup of ^{7}Be are less than about 1% of that of elastic scattering for the scattering angle of the c.m. of ^{7}Be, θ_7, below about 4°. In general θ_7 can differ from the ^{8}B scattering angle θ_8 in the ^{8}B+^{208}Pb $\to$ p+^{7}Be +^{208}Pb process, but the difference between the two angles is very small, since the energy transfer in the ^{8}B breakup concerned is much smaller than the incident energy of ^{8}B. These facts imply that in $\mathfrak{T}$ one can neglect matrix elements of $v_{\rm A7}$ between the ground state and excited states of ^{7}Be. One can, therefore, approximate $v_{\rm A7}$ by the single-folding potential

$$U_{\rm A7}(\mathbf{R}_{\rm A7})\equiv\langle\phi_7^{(0)}(\xi_7)|v_{\rm A7}(\mathbf{R}_{\rm A7},\xi_7)|\phi_7^{(0)}(\xi_7)\rangle_{\xi_7}.$$

Similarly, v_{17} can be approximated by

$$V_{17}(\mathbf{r})\equiv\langle\phi_7^{(0)}(\xi_7)|v_{17}(\mathbf{r},\xi_7)|\phi_7^{(0)}(\xi_7)\rangle_{\xi_7}.$$

In this approximation, $\mathfrak{T}$ is given by

$$\mathfrak{T}\approx\langle\chi_1\chi_7|U_{\rm A7}+U_{\rm A1}+V_{17}|\mathcal{O}\rangle \tag{3}$$

with

$$\mathcal{O}\equiv\langle\phi_7^{(0)}|\Psi\rangle. \tag{4}$$

If the incident momentum of the ^{8}B projectile is $\mathbf{P}$, one can make use of the well-known formula for Ψ and write

$$\mathcal{O}=\left\langle\phi_7^{(0)}\left|\frac{i\varepsilon}{E-H+i\varepsilon}\right|\phi_8^{(0)}e^{i\mathbf{P}\cdot\mathbf{R}}\right\rangle, \tag{5}$$

where H is the exact Hamiltonian of the system

$$H=T_r+T_R+V+h_7,$$

where T_r and T_R are the kinetic energy operators with respect to $\mathbf{r}$ and $\mathbf{R}$, respectively, and h_7 is the internal Hamiltonian of ^{7}Be. The total energy of the system is denoted by E, which is related to the c.m. incident energy of ^{8}B $E_{\rm in}$ by $E=E_{\rm in}+e_7+e_{17}$, where e_7 is the eigenenergy of $\phi_7^{(0)}$ and e_{17} is the relative energy between p and ^{7}Be in the ground state of ^{8}B. Under the assumption of the inert ^{7}Be nucleus mentioned above, one can approximate H in Eq. (5) by

$$H\approx e_7+H_{3\text{-body}}, \tag{6}$$

where $H_{3\text{-body}}$ is the p+^{7}Be+A three-body Hamiltonian defined by

$$H_{3\text{-body}}=T_r+T_R+V_{17}(\mathbf{r})+U_{\rm A7}(\mathbf{R}_{\rm A7})+U_{\rm A1}(\mathbf{R}_{\rm A1}). \tag{7}$$

Consequently,

$$\mathfrak{T}\approx\left\langle\chi_1\chi_7\middle|U_{\rm A7}+U_{\rm A1}+V_{17}\middle|\Omega^{(+)}\varphi^{(0)}(\mathbf{r})e^{i\mathbf{P}\cdot\mathbf{R}}\right\rangle, \tag{8}$$

where

$$\Omega^{(+)}\equiv\frac{i\varepsilon}{E-e_7-H_{3\text{-body}}+i\varepsilon} \tag{9}$$

is Mϕller's wave matrix with the outgoing boundary condition and

$$\varphi^{(0)}(\mathbf{r})\equiv\langle\phi_7^{(0)}(\xi_7)|\phi_8^{(0)}(\xi_7,\mathbf{r})\rangle_{\xi_7} \tag{10}$$

is the overlap function between the ground state wave functions of ^{7}Be and ^{8}B. As one sees from Eq. (8), $\varphi^{(0)}(\mathbf{r})$ plays an essential role in the T-matrix element. Its calculation, however, requires the wave functions of the two nuclei that are not readily available. We, therefore, substitute it by a constant $\mathfrak{S}_{\rm exp}^{1/2}$ times a physically plausible normalized function $f^{(0)}(\mathbf{r})$. In this work we take it to be a solution of

$$(T_r + \tilde{V}_{17}(\mathbf{r}) - e_{17}) f^{(0)}(\mathbf{r}) = 0, \tag{11}$$

where $\tilde{V}_{17}(\mathbf{r})$ is a Woods-Saxon potential that is supposed to represent the single-particle potential of p in ^{8}B. Since the norm of $\varphi^{(0)}(\mathbf{r})$ is the spectroscopic factor of p in ^{8}B, $\mathfrak{S}_{\rm exp}$ is its approximation if $f^{(0)}(\mathbf{r})$ is close to $\varphi^{(0)}(\mathbf{r})/||\varphi^{(0)}(\mathbf{r})||^{1/2}$. After the substitution of $f^{(0)}(\mathbf{r})$, the T-matrix element becomes

$$\begin{aligned} \mathfrak{T} &\approx \mathfrak{S}_{\rm exp}^{1/2} \mathfrak{T}^{\rm 3\text{-}body}, \\ \mathfrak{T}^{\rm 3\text{-}body} &\equiv \langle \chi_1 \chi_7 | U_{\rm A7} + U_{\rm A1} + V_{17} | \Psi_{\rm 3\text{-}body} \rangle, \end{aligned} \tag{12}$$

where

$$\Psi_{\rm 3\text{-}body} = \Omega^{(+)} f^{(0)}(\mathbf{r}) e^{i\mathbf{P}\cdot\mathbf{R}} \tag{13}$$

is the wave function of the total system with incident wave of ^{8}B consisting of a proton and an inert ^{7}Be bound in a state $f^{(0)}(\mathbf{r})$ impinging on the target with momentum $\mathbf{P}$.

Thus, in the particular case under consideration, the exact T-matrix element can approximately be calculated by three-body CDCC. Furthermore, since the reaction is peripheral in r as already mentioned, the radial part of $f^{(0)}(\mathbf{r})$ in $\mathfrak{T}^{\rm 3\text{-}body}$ can be replaced by its asymptotic form

$$f_{\rm r}^{(0)}(r) \sim \alpha W_{-\eta,3/2}(2k_0 r)/r. \tag{14}$$

Thus, $\mathfrak{T}$ is approximately proportional to

$$C = \mathfrak{S}_{\rm exp}^{1/2} \alpha. \tag{15}$$

From the definitions of $\mathfrak{S}_{\rm exp}^{1/2}$ and α, it is clear that C is in good approximation the ratio of $\varphi_{\rm r}^{(0)}(r)$ to $W_{-\eta,3/2}(2k_0 r)/r$, i.e. the ANC of $\varphi_{\rm r}^{(0)}(r)$ we look for. Thus, one sees that the cross section is indeed proportional to C^2. It should be noted that this proportionality holds only when the reaction is peripheral in r, which is indeed the case for the ^{8}B breakup concerned.

In practice, we calculate the cross section $\sigma_{\rm calc}$ from $\mathfrak{T}^{\rm 3\text{-}body}$ for each choice of $f^{(0)}(\mathbf{r})$ with the three-body model CDCC as in the previous work [15, 16]. We then obtain $\mathfrak{S}_{\rm exp}$ by taking the ratio of the measured cross section to $\sigma_{\rm calc}$. Since the amplitude α is readily known, the ANC, C, can then be calculated by Eq. (15). It should be noted that, since $f^{(0)}(\mathbf{r})$ and $\varphi^{(0)}(\mathbf{r})$ may have quite different forms in the inner region, $\mathfrak{S}_{\rm exp}^{1/2}$ may be quite different from the true spectroscopic amplitude, $||\varphi^{(0)}(\mathbf{r})||^{1/2}$, and depend strongly on the choice of $f^0(\mathbf{r})$. In contrast, C given by Eq. (15) is independent of $f^{(0)}(\mathbf{r})$ and exactly the ANC of $\varphi^{(0)}(\mathbf{r})$ if the ^{8}B breakup reaction is genuinely peripheral with no contribution of the inner part of the ^{8}B wave function. Once C is well determined from a peripheral reaction, $S_{17}(0)$ can be obtained by [34]

$$S_{17}(0) \approx 38.0(1 - 0.0013\bar{a}_{\rm s})C^2, \tag{16}$$

where $\bar{a}_{\rm s}$ is the s-wave p-^{7}Be scattering length that can be calculated by the p-^{7}Be interaction potential used in the analysis. The accuracy of the $S_{17}(0)$ extracted with the ANC method can quantitatively evaluated by the dependence of C on the choice of $f^{(0)}(\mathbf{r})$, as shown in Sec. III C.

Thus, we see that $S_{17}(0)$ can be extracted from the CDCC analysis of ^{8}B breakup based on the p+^{7}Be+A three-body model, if one concentrates on the ^{8}B breakup into forward angles, i.e. $\theta_8 \lesssim 4^\circ$.

B. E-CDCC and hybrid scattering amplitude

In this subsection we describe the formalism of E-CDCC and how to construct a hybrid scattering amplitude from the results of E-CDCC and fully quantum-mechanical CDCC. The following formulation contains two important extensions of E-CDCC. One is the inclusion of the intrinsic spins of the projectile and its constituent fragments and the other is a more accurate treatment of the Coulomb wave function in the coupled-channel equations than in the previous formulation of E-CDCC [30]. Detailed formalism of CDCC and its theoretical foundations are given elsewhere [15, 16, 35].

As already mentioned in Sec. II A, the total wave function $\Psi_{\rm 3\text{-}body}$ of the p+^{7}Be+A three-body system satisfies the three-body Schrödinger equation,

$$(H_{\rm 3\text{-}body} - E_{\rm in} - e_{17}) \Psi_{\rm 3\text{-}body}(\mathbf{R}, \mathbf{r}) = 0. \tag{17}$$

In this model, the ^{8}B nucleus is assumed to consist of a ^{7}Be core in its ground state and a proton moving around it. Its intrinsic wave function, therefore, has the form $\Phi_{i,\ell SIm}(\mathbf{r})$ where ℓ is the orbital angular momentum of relative motion between p and ^{7}Be, S is the channel spin, and I and m are, respectively, the total angular momentum of ^{8}B and its z-component. The z-axis is taken to be parallel to the incident beam. The index i stands for the i th of the states with the quantum numbers $\{\ell,\, S,\, I,\, m\}$. For simplicity we denote below the five channel-indices $\{i,\, \ell,\, S,\, I,\, m\}$ as c. The set $\{\Phi_c\}$ consists of bound-states and "discretized-continuum-states" as in Refs. [15, 16]. For the calculation of the latter, the average method [15, 16, 18, 36] and the pseudo-state methods [15, 37, 38, 39] are widely used. In the present work, we assume that the Φ_c satisfy

$$\langle \Phi_{c'}(\mathbf{r}) | h | \Phi_c(\mathbf{r}) \rangle_{\mathbf{r}} = \epsilon_{i,\ell SI} \delta_{c'c}, \tag{18}$$

where h is the internal Hamiltonian of ^{8}B given by $h = T_r + \tilde{V}_{17}(\mathbf{r})$, and $\epsilon_{i,\ell SI}$ is the intrinsic energy corresponding to the channel $\{i,\, \ell,\, S,\, I\}$. We take the following scheme of angular momentum coupling for $\Phi_c(\mathbf{r})$

$$\begin{aligned} \Phi_c(\mathbf{r}) &= \varphi_{i,\ell SI}(r) \sum_{m_\ell, m_S} (\ell m_\ell S m_S | Im) i^\ell Y_{\ell m_\ell}(\hat{\mathbf{r}}) \zeta_{S m_S} \\ &\equiv \varphi_{i,\ell SI}(r) \left[i^\ell Y_\ell(\hat{\mathbf{r}}) \otimes \zeta_S \right]_{Im}, \end{aligned} \tag{19}$$

where $Y_{\ell m_\ell}$ is the spherical harmonics and $\zeta_{S m_S}$ is the spin wave function of ^{8}B with channel spin S.

We expand $\Psi_{3\text{-body}}$ in terms of the $\Phi_c(\mathbf{r})$ as

$$\Psi_{3\text{-body}}(\mathbf{R},\mathbf{r}) = \sum_c \Phi_c(\mathbf{r}) e^{-i(m-m_0)\phi_R} \chi_c(R,\theta_R), \quad (20)$$

where the coefficient $\chi_c(R,\theta_R)\exp[-i(m-m_0)\phi_R]$ of the expansion describes the c.m. motion of the projectile relative to A in channel c, and m_0 is m in the initial state. Since the Φ_c are chosen to form an approximate complete set in a finite region of space that is important for the reaction concerned [37], the expansion of Eq. (20) is accurate in that region of space. Unknown coefficients χ_c of the expansion are obtained by solving coupled-channel equations derived below.

Multiplying Eq. (17) by $\Phi^*_{c'}(\mathbf{r})$ from the left, integrating over $\mathbf{r}$, and summing over the spin states, one obtains the coupled equations for the χ_c

$$\begin{aligned} e^{-im'\phi_R}(\mathcal{T}_R + \epsilon_{i',\ell'S'I'} - E_{\rm in} - e_{17})\chi_{c'}(R,\theta_R) \\ = -\sum_c F_{c'c} e^{-im\phi_R}\chi_c(R,\theta_R), \quad (21) \end{aligned}$$

where $\mathcal{T}_R$ is the reduced kinetic energy operator defined by

$$\mathcal{T}_R = -\frac{\hbar^2}{2\mu}\left[\frac{1}{b}\frac{\partial}{\partial b}\left(b\frac{\partial}{\partial b}\right) + \frac{\partial^2}{\partial z^2}\right] + \frac{\hbar^2}{2\mu}\frac{(m'-m_0)^2}{b^2} \quad (22)$$

in the cylindrical coordinates $\mathbf{R} = (z, b, \phi_R)$. The impact parameter of the collision, b, is defined by $b = \sqrt{x^2+y^2}$ with $\mathbf{R} = (x,y,z)$ in the Cartesian coordinate. The two arguments of χ_c in Eq. (21) are given by $R = \sqrt{z^2+b^2}$ and $\theta_R = \cos^{-1}(z/\sqrt{z^2+b^2})$. In Eq. (22) μ is the reduced mass of the ^{8}B-A system. In the peripheral region, in which b is large, we neglect the last term of the r.h.s. of Eq. (22), which turns out to have no effect on numerical results in the present case. Thus,

$$\mathcal{T}_R \approx -\frac{\hbar^2}{2\mu}\left[\frac{1}{b}\frac{\partial}{\partial b}\left(b\frac{\partial}{\partial b}\right) + \frac{\partial^2}{\partial z^2}\right] \equiv \mathcal{T}'_R. \quad (23)$$

The form factor $F_{c'c}$ in Eq. (21) of the coupling between channels c and c' is given by

$$\begin{aligned} F_{c'c}(\mathbf{R}) &= \langle \Phi_{c'} | U_{\rm A7} + U_{\rm A1} | \Phi_c \rangle_{\mathbf{r}} \\ &\equiv \mathcal{F}_{c'c}(R,\theta_R) e^{-i(m'-m)\phi_R}, \quad (24) \end{aligned}$$

where we assume $U_{\rm A7}$ and $U_{\rm A1}$ to be central potentials. This assumption is valid as discussed in Ref. [30] since we use E-CDCC only to obtain the scattering amplitude for large values of b. The multipole expansion of $\mathcal{F}_{c'c}$ is obtained from those of the coupling potentials

$$\begin{aligned} U_{\rm A7}(R_{\rm A7}) &= \sum_\lambda u^{(\lambda)}_{\rm A7}(R, r/8)\frac{4\pi}{\hat{\lambda}^2}\sum_\nu Y^*_{\lambda\nu}(\hat{\mathbf{R}})Y_{\lambda\nu}(\hat{\mathbf{r}}), \\ U_{\rm A1}(R_{\rm A1}) &= \sum_\lambda u^{(\lambda)}_{\rm A1}(R, 7r/8)\frac{4\pi}{\hat{\lambda}^2}\sum_\nu Y^*_{\lambda\nu}(\hat{\mathbf{R}})Y_{\lambda\nu}(\hat{\mathbf{r}}). \end{aligned}$$

Then, $\mathcal{F}_{c'c}$ can be expanded as

$$\begin{aligned} \mathcal{F}_{c'c}(R,\theta_R) &= \sum_\lambda i^{\ell-\ell'}\sqrt{4\pi}(-)^{2I'+m-S} \\ &\times \sqrt{\frac{(2\ell+1)(2\ell'+1)(2I+1)(2I'+1)}{(2\lambda+1)^3}} \\ &\times (I\,-m\,I'm'|\lambda\,m'{-}m)(\ell 0\ell' 0|\lambda 0) \\ &\times W(\ell\ell' II';\lambda S)\delta_{S'S} \\ &\times C_{\lambda\,m'-m}P_{\lambda\,m'-m}(\cos\theta_R) \\ &\times \int \varphi^*_{i',\ell'S'I'}(r)\mathcal{U}^{(\lambda)}(R,r)\varphi_{i,\ell SI}(r) r^2 dr, \end{aligned}$$

where $W(\ell\ell' II';\lambda S)$ is the Racah coefficient,

$$C_{\lambda\nu} \equiv (-)^{(\nu+|\nu|)/2}\sqrt{\frac{2\lambda+1}{4\pi}\frac{(\lambda-|\nu|)!}{(\lambda+|\nu|)!}},$$

and $\mathcal{U}^{(\lambda)}(R,r) = u^{(\lambda)}_{\rm A7}(R,r/8) + u^{(\lambda)}_{\rm A1}(R,7r/8)$.

Now we make the Coulomb-eikonal approximation [40] to χ_c:

$$\chi_c(R,\theta_R) \approx \psi_c(b,z)\phi^{\rm C(+)}_c(b,z), \quad (25)$$

where $\phi^{\rm C(+)}_c$ is the Coulomb wave function with outgoing scattered wave and ψ_c is the function to be determined with the Eikonal approximation. The Coulomb wave functions are given by

$$\begin{aligned} \phi^{\rm C(+)}_c(b,z) &= \frac{e^{-\pi\eta_c/2}}{(2\pi)^{3/2}}\Gamma(1+i\eta_c)e^{i\mathbf{K}_c\cdot\mathbf{R}}F^c_{\mathbf{K}_c}(\mathbf{R}), \\ F^c_{\mathbf{K}_c}(\mathbf{R}) &\equiv G(-i\eta_c, 1, i(K_cR - \mathbf{K}_c\cdot\mathbf{R})) \end{aligned}$$

with Γ the Gamma function and G the confluent hypergeometric function. In actual calculation we make use of the approximate asymptotic-form of $\phi^{\rm C(+)}_c$,

$$\begin{aligned} \phi^{\rm C(+)}_c(b,z) &\sim \frac{1}{(2\pi)^{3/2}}\left(1 + \frac{\eta_c^2}{i(K_cR - \mathbf{K}_c\cdot\mathbf{R})} + ...\right) \\ &\quad \times e^{i(\mathbf{K}_c\cdot\mathbf{R}+\eta_c\ln(K_cR-\mathbf{K}_c\cdot\mathbf{R}))} \\ &\approx \frac{1}{(2\pi)^{3/2}}e^{i(K_cz+\eta_c\ln(K_cR-K_cz))}, \quad (26) \end{aligned}$$

which is valid for large values of b. The boundary condition for ψ_c in Eq. (25) is $\lim_{z\to-\infty}\psi_c(b,z) = \delta_{c0}$, where 0 denotes the incident channel, so that χ_c satisfies the appropriate boundary condition $\lim_{z\to-\infty}\chi_c(R,\theta_R) = \delta_{c0}\phi^{\rm C(+)}_c(b,z)$.

We make the following two approximations as in Ref. [30]. (i) For sufficiently large b, the flux of $\phi^{\rm C(+)}_c$ is parallel to the z-axis. (ii) Local semiclassical approximation [41] to $\phi^{\rm C(+)}_c$,

$$\frac{\partial\phi^{\rm C(+)}_c(b,z)}{\partial z} \approx iK_c(R)\phi^{\rm C(+)}_c(R), \quad (27)$$

which is valid for a wave function in a slowly-varying potential. The local momentum $K_c(R)$ is defined by

$$\frac{\hbar^2}{2\mu}K^2_c(R) = E_{\rm in} + e_{17} - \epsilon_{i,\ell SI} - \frac{Z_8Z_{\rm A}e^2}{R}, \quad (28)$$

where $Z_8 e$ ($Z_{\rm A} e$) represents the charge of ^{8}B (A). Further approximation to $\phi_c^{\rm C(+)}$ was made in Ref. [30], i.e. the c-dependence of $F^c_{{\bf K}_c}$ was neglected. In the present paper, however, we take account of that dependence using Eq. (26). This treatment of the Coulomb wave function slightly improves the agreement between the quantum-mechanical and eikonal scattering-amplitudes for large orbital angular momentum L of ^{8}B-A relative motion. The explicit forms of the two amplitudes are given later in Eqs. (37)–(40).

With Eq. (23) and the Coulomb-eikonal approximation, we obtain

$$\begin{aligned}\mathcal{T}_R \chi_c^J(R,\theta_R) &\approx \mathcal{T}'_R \left(\psi_c(b,z)\phi_c^{\rm C(+)}(b,z)\right) \\ &\approx \Bigg[-\frac{i\hbar^2}{\mu} K_c(R) \left(\frac{\partial \psi_c(b,z)}{\partial z}\right) \phi_c^{\rm C(+)}(b,z) \\ &\quad + \left(\mathcal{T}'_R \phi_c^{\rm C(+)}(b,z)\right) \psi_c(b,z) \Bigg],\end{aligned} \tag{29}$$

where the second-order derivative of ψ_c is neglected since it is slowly varying compared with $\phi_c^{\rm C(+)}$. Inserting Eqs. (24), (26), (29), and

$$\begin{aligned}\mathcal{T}'_R \phi_c^{\rm C(+)}(b,z) &= \left(E_{\rm in} + e_{17} - \epsilon_{i,\ell SI} - \frac{Z_8 Z_{\rm A} e^2}{R}\right) \\ &\quad \times \phi_c^{\rm C(+)}(b,z)\end{aligned}$$

into Eq. (21), we arrive at the following coupled-channel equations

$$\begin{aligned}\frac{i\hbar^2}{\mu} K_c(R) \frac{d}{dz} \psi_c^{(b)}(z) &= \sum_{c'} \mathfrak{F}^{(b)}_{cc'}(z)\, \mathcal{R}^{(b)}_{cc'}(z)\, \psi^{(b)}_{c'}(z) \\ &\quad \times e^{i(K_{c'}-K_c)z},\end{aligned} \tag{30}$$

where the non-dynamical variable b is put in a superscript, the reduced coupling-potential $\mathfrak{F}_{cc'}$ is defined by

$$\mathfrak{F}^{(b)}_{cc'}(z) = \mathcal{F}^{(b)}_{cc'}(z) - \frac{Z_8 Z_{\rm A} e^2}{R} \delta_{cc'}, \tag{31}$$

and

$$\mathcal{R}^{(b)}_{cc'}(z) \equiv \frac{e^{i\eta_{c'} \ln{(K_{c'}R - K_{c'}z)}}}{e^{i\eta_c \ln{(K_c R - K_c z)}}} = \frac{(K_{c'}R - K_{c'}z)^{i\eta_{c'}}}{(K_c R - K_c z)^{i\eta_c}}.$$

Since Eq. (30) is a set of first-order differential equations and contains no coefficient with very large angular momentum L, one can solve it with high computational speed and accuracy.

The eikonal scattering amplitude with Coulomb distortion is given by $f^{\rm E}_{c0} = f^{\rm Ruth}_{c0}\delta_{c0} + f'^{\rm E}_{c0}$, where $f^{\rm Ruth}_{c0}$ is the Rutherford amplitude and

$$\begin{aligned}f'^{\rm E}_{c0} &\equiv -\frac{(2\pi)^2\mu}{\hbar^2} \int \sum_{c'} \mathfrak{F}^{(b)}_{cc'}(z)\, \phi_c^{*\rm C(-)}(b,z) \phi_{c'}^{\rm C(+)}(b,z) \\ &\quad \times e^{-i(m-m_0)\phi_R}\, \psi^{(b)}_{c'}(z) d{\bf R}\end{aligned} \tag{32}$$

with

$$\begin{aligned}\phi_c^{\rm C(-)}(b,z) &= \frac{e^{-\pi\eta_c/2}}{(2\pi)^{3/2}} \Gamma^*(1+i\eta_c) e^{i{\bf K}'_c\cdot{\bf R}} F^{c*}_{-{\bf K}'_c}({\bf R}) \\ &\approx \frac{1}{(2\pi)^{3/2}} e^{i{\bf K}'_c\cdot{\bf R}} e^{-i\eta_c \ln{(K_c R + {\bf K}'_c\cdot{\bf R})}}.\end{aligned} \tag{33}$$

The outgoing c.m. momentum ${\bf K}'_c$ is chosen to be on the z-x plane, following the Madison convention. For forward scattering in which ${\bf K}'_c$ is almost parallel to ${\bf K}_{c'}$, i.e. to the z-axis, we approximate, in the same way as in Ref. [30], the phase-factor $({\bf K}_{c'} - {\bf K}'_c)\cdot{\bf R}$, which appears in $\phi_c^{*\rm C(-)}(b,z)\phi_{c'}^{\rm C(+)}(b,z)$, by $-K_c\theta_f b \cos\phi_R + (K_{c'} - K_c)z$, where θ_f is the scattering angle of ^{8}B, and $K_c R + {\bf K}'_c \cdot {\bf R}$ in Eq. (33) by $K_c R + K_c z$. Under these approximations,

$$\begin{aligned}f'^{\rm E}_{c0} &\approx -\frac{\mu}{2\pi\hbar^2} \int e^{-i(m-m_0)\phi_R} e^{-iK_c \sin\theta_f b \cos\phi_R}\, b db d\phi_R \\ &\quad \times \mathcal{H}^{(b)}_c \int \sum_{c'} \mathfrak{F}^{(b)}_{cc'}(z)\, \psi^{(b)}_{c'}(z)\, e^{i(K_{c'}-K_c)z} \mathcal{R}^{(b)}_{cc'}(z) dz\end{aligned} \tag{34}$$

with $\mathcal{H}^{(b)}_c \equiv \exp[2i\eta_c \ln{(K_c b)}]$.

The integration over z in Eq. (34) can be done analytically with the help of Eq. (30), with the result

$$\begin{aligned}\mathcal{I} &\equiv \int \sum_{c'} \mathfrak{F}^{(b)}_{cc'}(z)\, \psi^{(b)}_{c'}(z)\, e^{i(K_{c'}-K_c)z} \mathcal{R}^{(b)}_{cc'}(z) dz \\ &= \frac{i\hbar^2}{\mu} \int K_c(R) \left(\frac{d}{dz}\psi^{(b)}_c(z)\right) dz \\ &\approx \frac{i\hbar^2}{\mu} \left[K_c(R)\psi^{(b)}_c(z)\right]^{\infty}_{-\infty} \\ &\equiv \frac{i\hbar^2}{\mu} K_c \left[\mathcal{S}^{(b)}_{c0} - \delta_{c0}\right],\end{aligned} \tag{35}$$

where $\partial K_c(R)/\partial z$ is neglected, since $K_c(R)$, with large b, is a slowly-varying function of z. The eikonal S-matrix elements are defined by $\mathcal{S}^{(b)}_{c0} = \lim_{z\to\infty} \psi^{(b)}_c(z)$. Insertion of Eq. (35) into Eq. (34) leads to

$$\begin{aligned}f'^{\rm E}_{c0} &\approx \frac{K_c}{2\pi i} \int e^{-i(m-m_0)\phi_R} e^{-iK_c \sin\theta_f b \cos\phi_R}\, b db d\phi_R \\ &\quad \times \mathcal{H}^{(b)}_c \left[\mathcal{S}^{(b)}_{c0} - \delta_{c0}\right].\end{aligned} \tag{36}$$

We now transform the integration over b to the summation over L as in Ref. [30]. The resulting eikonal scattering amplitude is

$$f^{\rm E}_{c0} = f^{\rm Ruth}_{c0}\delta_{c0} + \frac{2\pi}{iK_0} \sum_L f'^{\rm E}_{L;c0}\, Y_{L\, m-m_0}(\hat{\bf K}'), \tag{37}$$

where

$$f'^{\rm E}_{L;c0} \equiv \frac{K_0}{K_c} \mathcal{H}^{(b_{c;L})}_c \sqrt{\frac{2L+1}{4\pi}}\, i^{(m-m_0)} \left[\mathcal{S}^{(b_{c;L})}_{c0} - \delta_{c0}\right] \tag{38}$$

with $K_c b_{c;L} = L + 1/2$. The quantum mechanical scattering amplitude obtained by CDCC is given by

$$f^{\mathrm{Q}}_{c0} = f^{\mathrm{Ruth}}_{c0}\delta_{c0} + \frac{2\pi}{iK_0}\sum_{L} f'^{\mathrm{Q}}_{L;c0}\, Y_{L\,m-m_0}(\hat{\mathbf{K}}') \tag{39}$$

with

$$\begin{aligned} f'^{\mathrm{Q}}_{L;c0} \equiv & \sum_{J=|L-I|}^{L+I}\sum_{L_0=|J-I_0|}^{J+I_0}\sqrt{\frac{2L_0+1}{4\pi}} \\ & \times(I_0 m_0 L_0 0|J m_0)(ImL\; m_0{-}m|J m_0) \\ & \times(S^{J}_{iL\ell SI,i_0L_0\ell_0S_0I_0} - \delta_{ii_0}\delta_{LL_0}\delta_{\ell\ell_0}\delta_{SS_0}\delta_{II_0}) \\ & \times e^{i(\sigma_L+\sigma_{L_0})}(-)^{m-m_0}, \end{aligned} \tag{40}$$

where σ_L is the Coulomb phase shift and J is the total angular momentum of the three-body system. We define the hybrid scattering amplitude by

$$\begin{aligned} f^{\mathrm{H}}_{c0} = & f^{\mathrm{Ruth}}_{c0}\delta_{c0} + \frac{2\pi}{iK_0}\sum_{L<L_{\mathrm{C}}} f'^{\mathrm{Q}}_{L;c0}\, Y_{L\,m-m_0}(\hat{\mathbf{K}}') \\ & + \frac{2\pi}{iK_0}\sum_{L\geq L_{\mathrm{C}}} f'^{\mathrm{E}}_{L;c0}\, Y_{L\,m-m_0}(\hat{\mathbf{K}}') \end{aligned} \tag{41}$$

and use it in the analysis of ^{8}B breakup.

The connecting-angular-momentum L_{C} between quantum mechanical and eikonal amplitudes is chosen so that $f^{\mathrm{E}}_{L;c0}$ agrees with $f^{\mathrm{Q}}_{L;c0}$ for $L \geq L_{\mathrm{C}}$. It should be noted that Eq. (41) includes all quantum effects and also the interference between amplitudes in the two L-regions. This hybrid CDCC calculation turns out to be capable of evaluating the nuclear and Coulomb breakup amplitudes with very high accuracy and computational speed. In fact, we have obtained the same accuracy as standard fully quantum mechanical CDCC calculations in about $1/10$ of computing time.

III. RESULTS AND DISCUSSION

A. Numerical calculation

For the wave functions of ^{8}B that form the basis of the CDCC expansion of the three-body system we make the following assumptions. We assume that the ground state wave function of ^{8}B, with the z-component m_0 of the total spin $I_0 = 2$ of it, is given by

$$\begin{aligned} f^{(0)}_{m_0}(\mathbf{r}) = & \{w_1\,[iY_1(\hat{\mathbf{r}})\otimes\zeta_1]_{2m_0} + w_2\,[iY_1(\hat{\mathbf{r}})\otimes\zeta_2]_{2m_0}\} \\ & \times f^{(0)}_{\mathrm{r}}(r) \\ \equiv & \; w_1 f^{(0)}_{1,m_0}(\mathbf{r}) + w_2 f^{(0)}_{2,m_0}(\mathbf{r}) \end{aligned} \tag{42}$$

in the channel spin representation, neglecting the $\ell \neq 1$ components. The values of the coefficients $w_1 \sim 0.397$ and $w_2 \sim 0.918$ are obtained from the result of the microscopic calculation [17] of ^{8}B, $C^2_{1/2}/C^2_{3/2} = 0.157$, where $C_{1/2}$ ($C_{3/2}$) is the ANC in the proton spin-orbit coupling representation corresponding to the $j \equiv |\vec{\ell} + \vec{\frac{1}{2}}| = 1/2$ (3/2) state. We further assume the effective p-^{7}Be interaction for the ground state of ^{8}B, $\tilde{V}^{(0)}_{17}$, to be independent of S, hence the same radial dependence $f^{(0)}_{\mathrm{r}}(r)$ of the $S = 1$ and $S = 2$ components in Eq. (42). This assumption is valid since only the tail region, $r > R_{\mathrm{N}}$, of $f^{(0)}(\mathbf{r})$ contributes to the ^{8}B breakup process concerned. The wave function of the p-^{7}Be scattering state with outgoing scattered waves is given by

$$f^{(+)}_{S,m_S}(\mathbf{k},\mathbf{r}) = \frac{i\varepsilon}{\varepsilon_{17} - T_r - V_{17} + i\varepsilon} e^{i\mathbf{k}\cdot\mathbf{r}}\zeta_{S,m_S}, \quad S = 1 \text{ or } 2, \tag{43}$$

where $e^{i\mathbf{k}\cdot\mathbf{r}}\zeta_{S,m_S}$ is the incident wave with definite channel spin S and its z-component m_S, ε_{17} is the incident energy in the c.m. frame of the p-^{7}Be system, and $\mathbf{k}$ is the incident momentum. The wave function with incoming scattered waves $f^{(-)}_{S,m_S}(\mathbf{k},\mathbf{r})$ corresponding to $f^{(+)}_{S,m_S}(\mathbf{k},\mathbf{r})$ used below is defined by $f^{(-)}_{S,m_S}(\mathbf{k},\mathbf{r}) = f^{(+)*}_{S,-m_S}(-\mathbf{k},\mathbf{r})$.

We assume that V_{17} has no tensor force component. We consider the breakup of ^{8}B to its scattering states at low ε_{17}, and truncate the modelspace by $\varepsilon_{17} \leq 10$ MeV. In the experiment we analyze, however, the cross section is measured for ε_{17} in the range of 500 keV $\leq \varepsilon_{17} \leq$ 750 keV, and it turns out that only coupling of those states with ε_{17} much lower than 10MeV need be taken into account as described in Sec. III B, for which only s-waves are affected by the nuclear part of V_{17}. All the higher partial waves have negligible amplitude inside its range because of the Coulomb and centrifugal barriers and there have no coupling with the s-waves. Therefore, all the angular momenta ℓ, S and I are conserved in $f^{(\pm)}_{S,m_S}(\mathbf{k},\mathbf{r})$. The channel spin S is conserved also in s-waves since $S = I$ that is a good quantum number. Thus, one sees that $f^{(+)}_{S,m_S}(\mathbf{k},\mathbf{r})$ is the pure state of S, while ℓ and I are mixed as in the incident wave $e^{i\mathbf{k}\cdot\mathbf{r}}$. It should be noted, however, that V_{17} for the s-waves depends on S as is evident from the large S-dependence of the s-wave p-^{7}Be scattering lengths: $a^{S=2}_{\mathrm{s}} = -7 \pm 3$ fm and $a^{S=1}_{\mathrm{s}} = 25 \pm 9$ fm [42].

Furthermore, it turns out that the spin-dependent part of the p-^{208}Pb optical potential has no effect on the resulting elastic cross section at forward angles. Thus, the channel spin S is conserved during the breakup process of ^{8}B by the ^{208}Pb target [15]. Under these circumstances, the S-dependent 3-body T-matrix element in actual CDCC calculation, $\mathfrak{T}^{\text{3-body}}_{S,m_Sm_0}$, is given by

$$\begin{aligned} \mathfrak{T}^{\text{3-body}}_{S,m_Sm_0} = & \; w_S\langle f^{(-)}_{Sm_S}(\mathbf{k},\mathbf{r})e^{i\mathbf{P}'\cdot\mathbf{R}}|U_{\mathrm{A7}} + U_{\mathrm{A1}} \\ & \times|\Omega^{(+)} f^{(0)}_{S,m_0}(\mathbf{r})e^{i\mathbf{P}\cdot\mathbf{R}}\rangle, \\ \equiv & \; w_S\mathfrak{T}'^{\text{3-body}}_{S,m_Sm_0}, \end{aligned} \tag{44}$$

where $\Omega^{(+)}$ is the wave matrix given in Eq. (9).

The unpolarized ^{8}B breakup cross section calculated by

CDCC, σ, is given by

$$\sigma = \frac{\mathcal{D}\rho}{2I_0+1}\sum_{m_0 m_1 m_7}\left|\sum_{S m_S}(\tfrac{1}{2}m_1\tfrac{3}{2}m_7|S m_S)w_S\mathfrak{T}'^{\text{3-body}}_{S,m_S m_0}\right|^2$$
$$= \frac{\mathcal{D}\rho}{2I_0+1}\sum_{S m_S m_0}w_S^2\left|\mathfrak{T}'^{\text{3-body}}_{S,m_S m_0}\right|^2 \equiv \sum_S w_S^2\sigma_S, \quad (45)$$

where m_1 (m_7) is the z-component of the spin of p (^{7}Be) and the orthonormality of the Clebsch-Gordan coefficient is used. We compare σ with the unpolarized cross sections measured by RIKEN experiment [7, 8, 9]. In the calculation of σ_1 and σ_2, we use an I-independent p-^{7}Be effective interaction $\tilde{V}_{17}$ as mentioned above. Then, the states of ^{8}B with fixed S and ℓ and different values of I are degenerate, which greatly simplifies numerical calculation. The value of $\bar{a}_{\rm s}$ in Eq. (16) corresponding to the spin-dependent ANC analysis is [34] $\bar{a}_{\rm s} = w_1^2 a_{\rm s}^{S=1} + w_2^2 a_{\rm s}^{S=2} \sim -2.8$ fm.

For $\tilde{V}_{17}^{(0)}$, the single-particle potential of Esbensen and Bertsch (EB) [43] is used, except that we neglect the spin-orbit part of the potential and adjust the depth of the central potential to reproduce the separation energy of p, 137 keV. The scattering states for the p-waves are also calculated with this $\tilde{V}_{17}^{(0)}$. For d- and f-states with both $S = 1$ and $S = 2$, we use the potential of Barker [44]. For the s-state in the $S = 2$ channel, we use the potential of Barker that gives the s-wave p-^{7}Be scattering length $a_{\rm s}^{S=2}$ of -8 fm. For the s-state with $S = 1$, we change the depth of the potential of Barker to 25.7 MeV so that the resulting scattering length $a_{\rm s}^{S=1}$ is 25 fm.

As for the distorting potential between p (^{7}Be) and ^{208}Pb we adopt the global optical potential by Koning and Delaroche [45] (Cook [46]). We neglect the spin-orbit parts of the p-^{208}Pb potential. The multipoles for nuclear and Coulomb coupling-potentials are included up to $\lambda = 6$. The discretized-continuum states of ^{8}B are constructed by the average method [15, 16, 18, 36]. The maximum excitation energy of ^{8}B is 10 MeV and 10, 20, 10, and 5 discretized-continuum states are taken for the $\ell = 1$, 0, 2, and 3 states, respectively. The resulting number of scattering-channels is 138. The maximum values of r, R, and L are, respectively, 200 fm, 1000 fm, and 12000. The modelspace described above turns out to give good convergence of the resulting breakup cross sections.

B. Analysis of ^{8}B breakup experiment

Figure 2 shows the convergence of the hybrid calculation with CDCC and E-CDCC for the breakup cross section of ^{8}B by ^{208}Pb at 52 MeV/nucleon. The cross section integrated over the excitation energy of ^{8}B measured from the p+^{7}Be threshold energy, ε_{17}, from 500 keV to 750 keV is plotted as a function of θ_8. The dashed line is the result of the E-CDCC calculation ($L_{\rm C} = 0$) and the dotted, dash-dotted, and solid lines correspond to the hybrid calculation with $L_{\rm C} =$ 500, 1000, and 1500, respectively. The figure shows that the hybrid calculation converges with $L_{\rm C} = 1000$. The difference between the dash-dotted and solid lines is only less than about 1% in magnitude. Thus, we regard the hybrid calculation of CDCC and E-CDCC with $L_{\rm C} = 1000$ as the fully quantum-mechanical CDCC calculation.

One sees in Fig. 2 the oscillation of the cross section at forward angles around 2°, which turns out to be due to the interference between nuclear and Coulomb breakup-amplitudes. Therefore, it can be concluded that nuclear interactions affect the breakup cross section even at very forward angles. However, as one sees below, this oscillation is not observed in actual experimental data because of the limit of the resolution of θ_8 in the measurement.

Figure 3 shows the comparison between CDCC calculation and the experimental data for the ^{8}B breakup. In order to take account of the experimental resolution and efficiency, the theoretical result has been smeared out by using the filtering table [47] provided by the authors of Ref. [8]. The upper panel shows the filtering effect on the cross section calculated with CDCC, where the solid and dashed lines represent the results obtained with and without the smearing procedure. In the lower panel, the smeared total breakup cross section is decomposed into the s- (dashed line), p- (dotted line), d- (dash-dotted line), and f-state (dash-two-dotted line) breakup components of ^{8}B.

One sees the smeared result of CDCC well agrees with the experimental data at forward angles ($\theta_8 \lesssim 4°$), while it underestimates the data at backward angles. The lower panel shows the importance of the p-state breakup for $\theta_8 \gtrsim 5°$, which implies that nuclear breakup is significant in this angular region. Thus, careful description of the p-state ^{8}B wave function, the resonance structures of it in particular, will be necessary to reproduce the experimental data at backward angles. The underestimation there may be due also to dynamical roles played by the excited-core component in ^{8}B, ^{7}Be($1/2^-$)$\otimes p$($3/2^-$), that is neglected in the present work as discussed in Sec. II A. Although further study in this line will be very interesting, it is

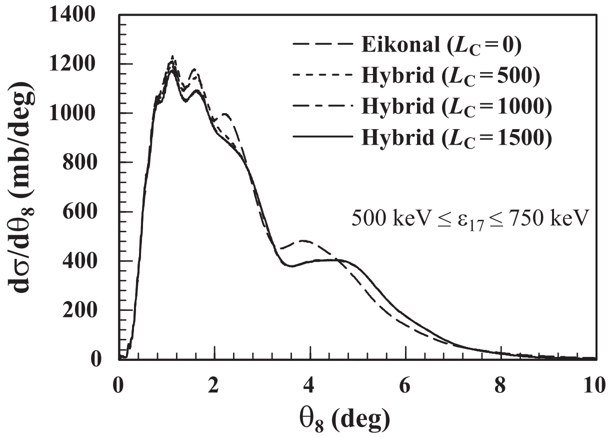

FIG. 2: The ^{8}B breakup cross section integrated over ε_{17} in the range of 500–750 keV, as a function of θ_8. The dotted, dash-dotted, and solid lines represent the results of the hybrid calculation of CDCC and E-CDCC with $L_{\rm C} = 500$, 1000, and 1500, respectively. The result of E-CDCC, i.e. $L_{\rm C} = 0$, is also shown by the dashed line.

beyond the scope of the present paper. Additionally, the filtering table used was made with assuming the s-state breakup of ^{8}B. Thus, quantitative comparison between the calculation and the experimental data, to extract $S_{17}(0)$ with high accuracy, can only be done in the region where the s-state breakup cross section is dominant. Therefore, below we use the data for $\theta_8 \le 4^\circ$ to determine $\mathfrak{S}_{\rm exp}$ by

$$\mathfrak{S}_{\rm exp} = \frac{\sigma_{\rm exp}}{\sigma}, \tag{46}$$

where σ is given by Eq. (45) and $\sigma_{\rm exp}$ is the corresponding experimental data.

Figure 4 shows the result of the χ^2-fit of the theoretical calculation to the experimental data. The solid line is the same as that in each panel in Fig. 3 but multiplied by the spectroscopic factor $\mathfrak{S}_{\rm exp} = 1.11$. The dashed line represents the result before being fitted, i.e. with $\mathfrak{S}_{\rm exp} = 1.00$. Each horizontal bar put on the eight data points below 4° does not represent a statistical error but it shows the range of θ_8 in which the breakup cross sections contribute to each data point [8]. The value of χ^2 per datum obtained is 8.5. Although the quality of the fit is not good, it should be noted that estimation of error-propagation in the present case, i.e. comparison between smeared experimental data and a smeared numerical result, is very complicated; the value of χ^2 per datum shown above takes account of no error with respect to θ_8. The value of α in Eq. (14) for the EB ^{8}B wave-function is 0.704 fm$^{-1/2}$. With the values of $\mathfrak{S}_{\rm exp}$ and α, the ANC C is obtained from Eq. (15) as $C = 0.740$ fm$^{-1/2}$. One can then determine $S_{17}(0)$ by inserting this result into Eq. (16), together with $\bar{a}_{\rm s} = -2.8$ fm, i.e. $S_{17}(0) = 20.9$ eV b. In the next subsection we quantitatively evaluate uncertainties of the extracted $S_{17}(0)$.

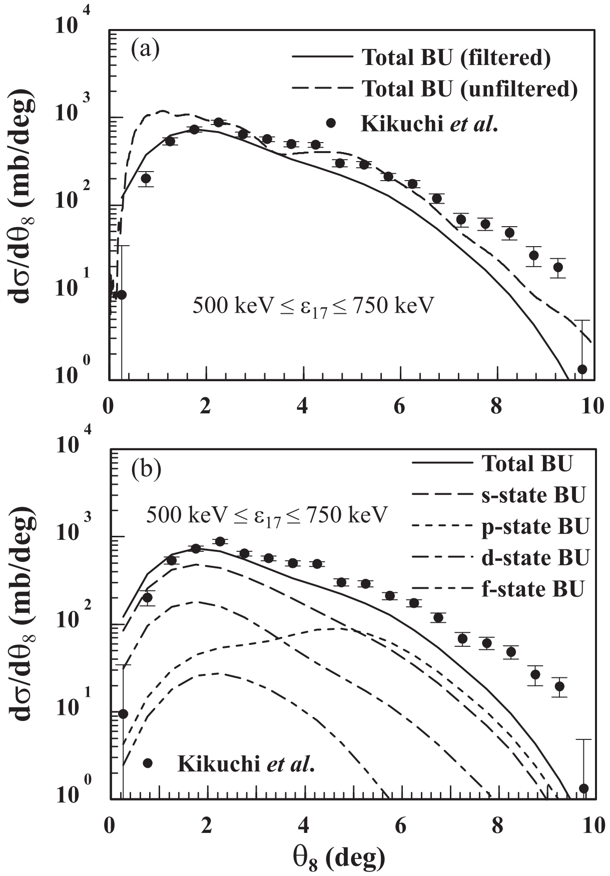

FIG. 3: (a) The calculated ^{8}B breakup cross sections with (solid line) and without (dashed line) the resolution and efficiency of the measurement [47] taken into account. The experimental data are taken from Ref. [8]. (b) Decomposition of the smeared ^{8}B breakup cross section into the s- (dashed line), p- (dotted line), d- (dash-dotted line), and f-state (dash-two-dotted line) breakup components.

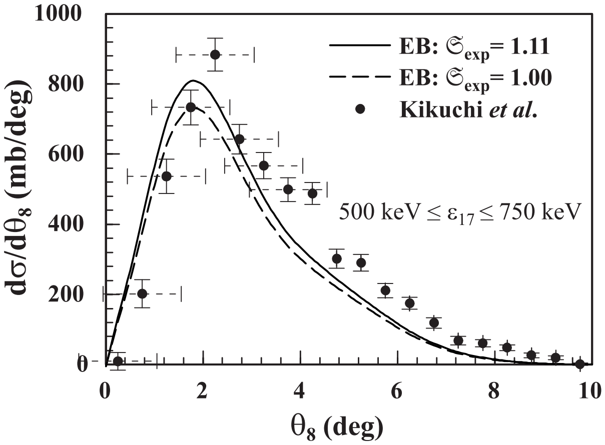

FIG. 4: The result of the χ^2-fit of the breakup cross section calculated with the ^{8}B single-particle potential of Esbensen and Bertsch (EB) [43]. The solid line is the same as that in each panel in Fig. 3 but multiplied by the spectroscopic factor $\mathfrak{S}_{\rm exp} = 1.11$. The result with $\mathfrak{S}_{\rm exp} = 1.00$ is also shown by the dashed line for comparison. For the eight data points below 4°, which are used in the fitting procedure, we have put the horizontal bar that represents the resolution of θ_8 [8] of the measurement.

C. Uncertainties of the extracted $S_{17}(0)$

First, we evaluate the uncertainty of $S_{17}(0)$ that comes from the use of the ANC method, just in the same way as in Refs. [26, 29]. We show in Fig. 5 the result of CDCC calculation with the p-state single-particle potential of ^{8}B by Kim *et al.* [48] (the dashed line) and that multiplied by $\mathfrak{S}_{\rm exp} = 0.867$ (the solid line); the latter agrees with the result shown in Fig. 4 within 1%. One sees that $\mathfrak{S}_{\rm exp}$ indeed depends on the p-state potential. Actually, α in Eq. (14) for Kim's potential is 0.796 fm$^{-1/2}$, which is quite different from the value for the EB potential, 0.704 fm$^{-1/2}$, because of the difference in the geometry of the two potentials of about 20%. On the contrary, the value of C in Eq. (15) calculated with Kim's potential is 0.741 fm$^{-1/2}$ that agrees very well with the result obtained with the EB potential shown in Sec. III B. This result shows that the ANC method works with very high accuracy in the

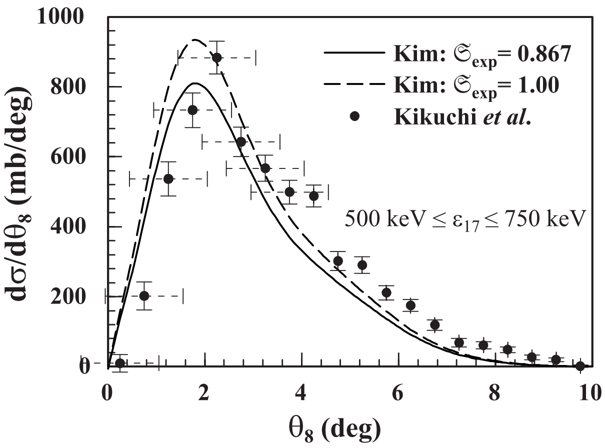

FIG. 5: Same as in Fig. 4 but for the CDCC calculation with Kim's single-particle potential [48] for the p-state of ^{8}B; the spectroscopic factor $\mathfrak{S}_{\rm exp}$ obtained is 0.867. The result with Kim's potential before χ^2-fitting, namely with $\mathfrak{S}_{\rm exp} = 1.00$, is also shown by the dashed line for comparison.

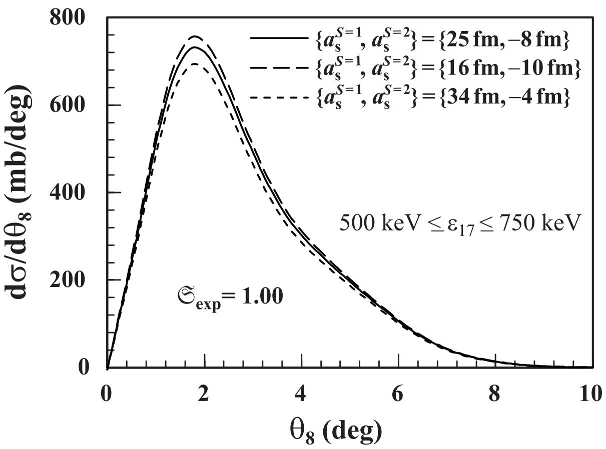

FIG. 6: Dependence of the ^{8}B breakup cross section on the s-state single-particle potentials of ^{8}B for the $S = 1$ and $S = 2$ channels. The solid line represents the result with the choice of the potentials that corresponds to the s-wave p-^{7}Be scattering lengths $\{a_{\rm s}^{S=1}, a_{\rm s}^{S=2}\} = \{25\ {\rm fm}, -8\ {\rm fm}\}$. The dashed (dotted) line shows the result with the s-state potentials corresponding to $\{a_{\rm s}^{S=1}, a_{\rm s}^{S=2}\} = \{16\ {\rm fm}, -10\ {\rm fm}\}$ ($\{34\ {\rm fm}, -4\ {\rm fm}\}$).

present analysis, i.e. the error of the ANC method is negligible.

Second, we estimate the effect of ambiguity of the distorting potentials used in the CDCC calculation on the obtained $S_{17}(0)$. For this purpose we use alternative optical potentials for p-^{208}Pb and ^{7}Be-^{208}Pb. For the p-^{208}Pb potential, we modify the parameter set of Koning and Delaroche so that the calculated elastic cross section without spin-orbit terms reproduces the one obtained with the full components of the optical potential. The parameter set thus obtained is $V_V = 39.82$ MeV, $W_V = 0.776$ MeV, and $W_D = 13.47$ MeV, with the same notation as in Ref. [45]; all other parameters are not changed. For the ^{7}Be-^{208}Pb potential, we use a single-folding model with the nucleon-^{208}Pb potential of Koning and Delaroche, neglecting the spin-orbit terms. The density distribution of ^{7}Be is assumed to be of the Gaussian form with the range that reproduces the rms matter radius of ^{7}Be of 2.48 fm [49]. The difference between the results calculated with the original and alternative optical potentials is found to be negligibly small (not shown). We conclude, therefore, that the error of $S_{17}(0)$ that comes from the ambiguity of the distorting potentials in the present case is negligibly small.

Finally, we estimate the uncertainty of $S_{17}(0)$ due to the ambiguity of the s-state single-particle potentials of ^{8}B for the $S = 1$ and $S = 2$ channels by changing the depth of the potential for the $S = 1$ ($S = 2$) channel ranging from 23.3 MeV (52.8 MeV) to 30.5 MeV (57.6 MeV), which gives the range of the resulting s-wave p-^{7}Be scattering length $a_{\rm s}^{S=1}$ ($a_{\rm s}^{S=2}$) from 16 fm (-10 fm) to 34 fm (-4 fm); these values of $a_{\rm s}^{S=1}$ and $a_{\rm s}^{S=2}$ are within the range of errors of the experimental values of them [42]. In Fig. 6 the solid, dashed, and dotted lines represent the results with the s-state potentials corresponding to $\{a_{\rm s}^{S=1}, a_{\rm s}^{S=2}\} = \{25\ {\rm fm}, -8\ {\rm fm}\}$, $\{16\ {\rm fm}, -10\ {\rm fm}\}$, and $\{34\ {\rm fm}, -4\ {\rm fm}\}$, respectively. One sees the breakup cross section slightly depends on the choice of the s-state potentials of ^{8}B; the resulting $S_{17}(0)$ is found to vary from 20.3 eV b to 21.9 eV b. Thus, we evaluate the error of $S_{17}(0)$ to be $+4.9\%/-2.9\%$.

Summarizing the discussion given above, the result of the present paper is as follows. The central value of $S_{17}(0)$ is 20.9 eV b. The theoretical error of the extracted $S_{17}(0)$ concerned with the s-wave p-^{7}Be scattering length is $+4.9\%/-2.9\%$. After including the 8.4% systematic experimental error, we obtain

$$S_{17}(0) = 20.9^{+1.0}_{-0.6}\ \text{(theo)} \pm 1.8\ \text{(expt)} \quad {\rm eVb}.$$

D. Discussion of the extracted $S_{17}(0)$

The main result of the present paper is $S_{17}(0) = 20.9^{+1.0}_{-0.6}$ (theo) ± 1.8 (expt) eV b derived from ^{208}Pb(^{8}B, p+^{7}Be)^{208}Pb at 52 MeV/nucleon. This value is significantly larger than $S_{17}(0) = 18.9 \pm 1.8$ eV b [9] obtained in the previous analysis of the same experiment with the first-order perturbation theory. In order to clarify the reason for the difference, we discuss roles of nuclear interaction, E2 transitions, and higher-order processes. In Fig. 7 the solid line is the same as in the upper panel in Fig. 3 that shows the result of full CDCC. The dashed line corresponds to the calculation without breakup components of nuclear coupling potentials. It should be noted that their diagonal components are included in the calculation to take account of the absorption of the flux of the incident particle by the target nucleus. One sees that the dashed line agrees with the solid line below 2° but deviates from it for $\theta_8 > 2^\circ$. As a result, the value of $S_{17}(0)$ obtained, $S_{17}(0) = 20.0^{+1.9}_{-1.8}$ eV b, is smaller than $S_{17}(0) = 20.9^{+1.0}_{-0.6}$ (theo) ± 1.8 (expt) eV b obtained with the full CDCC calculation mentioned above.

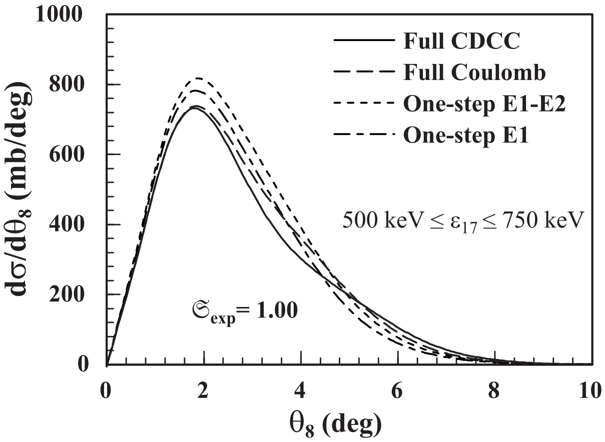

FIG. 7: Same as in Fig. 3 with different assumptions for CDCC. The lines represent the results of CDCC with nuclear and Coulomb couplings and all higher-order processes (solid line), CDCC without nuclear breakup (dashed line), one-step CDCC with Coulomb E1 and E2 components (dotted-line), and one-step CDCC with Coulomb E1 only that corresponds to the first-order virtual photon absorption theory (dash-dotted line).

The dash-dotted line in Fig. 7 represents the result of first-order iterative solutions of CDCC, designated as one-step CDCC, without nuclear breakup, including only $\lambda = 1$ (E1) component of the Coulomb interaction; this calculation is essentially the same as the first-order perturbation theory (virtual photon theory) used in the previous analysis of the experimental data [9]. It overestimates the solid line above 1.5° and the resulting value of $S_{17}(0)$ is $19.0^{+1.9}_{-1.7}$ eV b, which agrees well with the value 18.9 ± 1.8 eV b obtained in Ref. [9].

If one includes the $\lambda = 2$ (E2) component in the one-step CDCC calculation of Coulomb breakup, the dotted line in Fig. 7 is obtained; the coupling potentials with $\lambda = 2$ are artificially multiplied by 0.7, following the analysis of the MSU data [13]. One sees from Fig. 7 that inclusion of the reduced E2 component somewhat increases the breakup cross section, which results in further decrease of $S_{17}(0)$ to $S_{17}(0) = 17.9^{+1.7}_{-1.6}$ eV b. This result is consistent with the conclusion of Ref. [13], in which $S_{17}(0) = 17.8^{+1.4}_{-1.2}$ eV b was derived with first-order perturbation theory including both E1 and the reduced E2 components. If the E2 component is not scaled, the resulting value of $S_{17}(0)$ is 16.7 eV b. This value is about 20% less than the result of full CDCC, 20.9 eV b. The difference is due to the nuclear and higher-order Coulomb processes since the coupling potentials with $\lambda \geq 3$ are found to have little effect on the total breakup-cross-section at $\theta_8 \leq 4^\circ$.

Thus, description of ^{8}B breakup process with nuclear and Coulomb breakup processes of both the E1 and E2 transitions and higher-order processes is a key to solve a puzzle recognized so far of the discrepancy between the values of $S_{17}(0)$ extracted from direct p-capture reactions, $S_{17}(0) = 22.1 \pm 0.6$ (expt) ± 0.6 (theo) eV b, and indirect ^{8}B dissociation experiments. In order to clarify the role of these components in ^{8}B breakup reaction in general, it is necessary to carry out analyses to wider range of data, such as those measured at MSU [12, 13] and GSI [10, 11], including the data on other quantities than that dealt with in the present work. Analysis of parallel momentum ($p_{//}$) distribution of ^{7}Be-fragment after breakup of ^{8}B is particularly important, since the role of E2 component was determined from it [12, 13]. In the analysis in Ref. [13] the result of first-order perturbation theory with an adjustable parameter was compared with CDCC calculation that is essentially the same as in the present paper. Because of the agreement of the two results, it was concluded that higher order processes were unimportant without quantitative evaluation of the nuclear and higher-order Coulomb processes as done in the present work. Actually, the contribution is about 20% of the total as already described. A CDCC analysis of the $p_{//}$ distribution has been done by Mortimer *et al.* [28], where the dependence of the calculated result on the strength of the Coulomb $\lambda = 2$ (E2) coupling potentials was discussed. They found that the E2 potentials must be multiplied by 1.6 to reproduce the experimental data, although the origin of the enhancement was not clear. Therefore, further investigation of the accuracy of the enhancement factor 1.6 seems necessary. Unfortunately, filtering table for the MSU experiment is not available to the present authors. At this stage, therefore, we can quantitatively extract $S_{17}(0)$ with CDCC and the ANC method only from the ^{8}B breakup experiment done at RIKEN. Nevertheless, comparison of our pure theoretical result with that shown in Ref. [28] is very interesting, which will be a subject of our future work.

E. ANC analysis of the direct measurement

In this subsection we report on our application of the ANC method to the p-capture reaction, ^{7}Be$(p,\gamma)^8$B, at energies of 116–362 keV [4]. We assume direct capture of p by ^{7}Be to the ground state of ^{8}B by a pure E1 transition. A simple potential-model is assumed for the bound and the scattering states of the p+^{7}Be system, using the single-particle potential of Sec. III A. The s- and d-state components in the initial scattering-state wave-function are taken into account, and the intrinsic spins of p and ^{7}Be are included in the channel spin representation described in Sec. III A. In Fig. 8 the solid line shows the calculated S_{17} as a function of the incident energy $E_{\rm c.m.}$ of the reaction in the c.m. frame of the p-^{7}Be system . The plotted $S_{17}(E_{\rm c.m.})$ has been multiplied by the spectroscopic factor $\mathfrak{S}_{\rm exp} = 1.15$ obtained by the χ^2-fit to the data below 362 keV. The calculated $S_{17}(E_{\rm c.m.})$ is not reliable at high energies, say $E_{\rm c.m.} > 400$ keV, since the inner part of the ^{8}B wave function plays an important role. At low energies, however, the ANC method works very well and a reliable value of the ANC C, and consequently $S_{17}(0)$, can be derived from the χ^2-fitting procedure. The value of $S_{17}(0)$ thus obtained is 21.7 eV b. Uncertainties of the $S_{17}(0)$ are evaluated in the same way as in Sec. III C and found to be $+0.37/-0.24$ eV b, almost all of which is due to the ambiguity of the s-state potentials for the $S = 1$ and $S = 2$ channels of the p-^{7}Be system. Including the 2.3% systematic experimental error, we obtain the

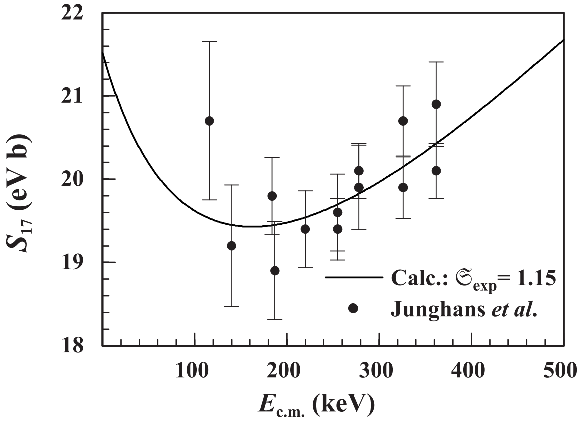

FIG. 8: The astrophysical factor S_{17} as a function of the incident energy $E_{\mathrm{c.m.}}$ of the reaction in the c.m. frame of the p-^{7}Be system. The solid line is the result of the calculation with a simple potential model, multiplied by $\mathfrak{S}_{\mathrm{exp}} = 1.15$. The experimental data are taken from Ref. [4].

following result: $S_{17}(0) = 21.7^{+0.37}_{-0.24}$ (theo) ±0.50 (expt) eV b. This result is consistent with both the value extracted from ^{8}B dissociation, $S_{17}(0) = 20.9^{+1.0}_{-0.6}$ (theo) ±1.8 (expt) eV b, described in the previous subsections, and the result obtained in Ref. [4], $S_{17}(0) = 22.1 \pm 0.6$ (expt) ±0.6 (theo) eV b, although no evaluation of the ambiguity due to the uncertainty of the s-wave p-^{7}Be scattering lengths, as the one described in Sec. III C, is made in Ref. [4].

IV. SUMMARY

The principal result of the present paper is the value of $S_{17}(0)$ of $20.9^{+1.0}_{-0.6}$ (theo) ±1.8 (expt) eV b obtained by an analysis of the cross section of the ^{8}B breakup reaction ^{208}Pb(^{8}B, p+^{7}Be)^{208}Pb at 52 MeV/nucleon measured at RIKEN [7, 8, 9] by means of the method of continuum-discretized coupled-channels [15, 16] (CDCC) combined with the asymptotic normalization coefficient (ANC) method [17]. The value is consistent with the one extracted from the precise measurement of the cross section of direct capture ^{7}Be(p, γ)^{8}B, $S_{17}(0) = 22.1 \pm 0.6$ (expt) ±0.6 (theo) eV b [4].

The CDCC calculation is based on the three-body model of p, ^{7}Be, and the target ^{208}Pb nucleus, with ^{7}Be staying in the ground state throughout the reaction process. This model is shown to be adequate in the breakup reaction in which the fragments p and ^{7}Be are ejected in very forward angles, less than 4°, which is the case for the experimental data analyzed in this work. Nuclear and Coulomb E1 and E2 transitions and multi-step processes of all-order are included in the calculation. The calculated cross section is shown to be proportional to the squared asymptotic amplitude of the overlap of the ground state wave functions of ^{7}Be and ^{8}B, which is a necessary condition for the applicability of the ANC method. The CDCC calculation is made efficient by the use of the eikonal CDCC method [30] (E-CDCC) for large angular momentum partial waves. Improvements of E-CDCC are made to cope with the Coulomb distortions of the incident and scattered waves of relative motion and intrinsic spins of the projectile and the ejectiles.

The main source of the error in the obtained $S_{17}(0)$ is the ambiguity of the s-wave p-^{7}Be interaction potentials for the channel spin $S = 1$ and $S = 2$ states. The errors associated with the use of the ANC method and the ambiguity of the distorting potentials are both negligible. Calculations of $S_{17}(0)$ with some simplified assumptions are summarized in Fig. 9. The results of first-order iterative solutions of CDCC, designated as one-step CDCC, correspond to and agree with those of first-order perturbation theory in the previous work [7, 8, 9, 12, 13]. The inclusion of the Coulomb quadrupole (E2) transitions, scaled by 0.7, in the one-step calculation decreases $S_{17}(0)$ by about 6%, and multistep processes increase it by about 20%. This shows the crucial importance of accurate description of the ^{8}B breakup process by CDCC including nuclear and Coulomb E1 and E2 transitions and all higher-order processes. It will be interesting to apply the method of the present paper to analyses of wider range of experiments such as those in Refs. [10, 11, 12, 13]. It may, however, be that the three-body CDCC used in the present paper is not valid in general and the use of CDCC with four-body model such as the one in Ref. [50] becomes necessary.

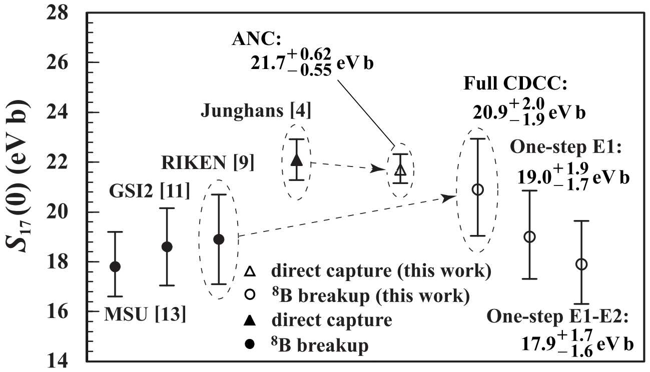

FIG. 9: The values of $S_{17}(0)$ extracted by the ANC method are shown by open symbols: the circles are obtained from three-types of CDCC analysis of ^{8}B breakup and the triangle is the result of analysis of ^{7}Be(p, γ)^{8}B with a simple potential model. The error of each result is obtained by adding the theoretical and experimental errors in quadrature. The results are compared with $S_{17}(0)$ extracted from the precise measurement of direct capture (p, γ) cross section [4] (closed triangle) and those obtained from ^{8}B dissociation with first-order perturbation theory (closed circles).

Acknowledgments

The authors would like to thank T. Motobayashi for helpful discussions and providing detailed information on the experiment. The authors also thank M. Kawai for fruitful discussions and careful reading of the manuscript. This work has been supported in part by the Grants-in-Aid for Scientific Research of Monbukagakusyou of Japan.

[1] J. N. Bahcall, M. H. Pinsonneault and Sarbani Basu, Astrophys. J. **555**, 990 (2001) and references therein.

[2] J. N. Bahcall, M. C. Gonzalez-Garcia and Carlos Peña-Garay, JHEP **0108**, 014 (2001) [arXiv:hep-ph/0106258]; JHEP **0302**, 009 (2003) [arXiv:hep-ph/0212147].

[3] J. N. Bahcall, Nucl. Phys. **B** Proc. Suppl. **118**, 77 (2003).

[4] A. R. Junghans *et al.*, Phys. Rev. C **68**, 065803 (2003).

[5] P. Descouvemont and D. Baye, Nucl. Phys. **A567**, 341 (1994).

[6] P. Descouvemont, Phys. Rev. C **70**, 065802 (2004).

[7] T. Motobayashi *et al.*, Phys. Rev. Lett. **73**, 2680 (1994);

[8] T. Kikuchi *et al.*, Phys. Lett. B **391**, 261 (1997).

[9] T. Kikuchi *et al.*, Eur. Phys. J. A **3**, 209 (1998).

[10] N. Iwasa *et al.*, Phys. Rev. Lett. **83**, 2910 (1999).

[11] F. Schümann *et al.*, Phys. Rev. Lett. **90**, 232501 (2003).

[12] B. Davids *et al.*, Phys. Rev. Lett. **86**, 2750 (2001).

[13] B. Davids *et al.*, Phys. Rev. C **63**, 065806 (2001).

[14] H. Esbensen, G. F. Bertsch and K. A. Snover, Phys. Rev. Lett. **94**, 042502 (2005).

[15] M. Kamimura *et al*., Prog. Theor. Phys. Suppl. **89**, 1 (1986).

[16] N. Austern *et al*., Phys. Reports. **154**, 125 (1987).

[17] A. M. Mukhamedzhanov and N. K. Timofeyuk, Yad. Fiz. **51**, 679 (1990) [Sov. J. Nucl. Phys. **51**, 431 (1990)]; H. M. Xu, C. A. Gagliardi, R. E. Tribble, A. M. Mukhamedzhanov and N. K. Timofeyuk, Phys. Rev. Lett. **73**, 2027 (1994).

[18] M. Yahiro, M. Nakano, Y. Iseri and M. Kamimura, Prog. Theor. Phys. **67**, 1467 (1982).

[19] M. Yahiro, Y. Iseri, M. Kamimura and M. Nakano, Phys. Lett. **141B**, 19 (1984).

[20] Y. Sakuragi and M. Kamimura, Phys. Lett. **149B**, 307 (1984) .

[21] Y. Sakuragi, Phys. Rev. C **35**, 2161 (1987).

[22] Y. Sakuragi, M. Kamimura and K. Katori, Phys. Lett. **B205**, 204 (1988); Y. Sakuragi, M. Yahiro, M. Kamimura and M. Tanifuji, Nucl. Phys. **A480**, 361 (1988).

[23] Y. Iseri, H. Kameyama, M. Kamimura, M. Yahiro and M. Tanifuji, Nucl. Phys. **A490**, 383 (1988).

[24] Y. Hirabayashi and Y. Sakuragi, Phys. Rev. Lett. **69**, 1892 (1992).

[25] J. A. Tostevin *et al*., Phys. Rev. C **66**, 024607 (2002); A. M. Moro, R. Crespo, F. Nunes and I. J. Thompson, Phys. Rev. C **66**, 024612 (2002) and references therein.

[26] K. Ogata, M. Yahiro, Y. Iseri and M. Kamimura, Phys. Rev. C **67**, 011602(R) (2003).

[27] J. A. Tostevin, F. M. Nunes and I. J. Thompson, Phys. Rev. C **63**, 024617 (2001).

[28] J. Mortimer, I. J. Thompson and J. A. Tostevin, Phys. Rev. C **65**, 064619 (2002).

[29] K. Ogata *et al.*, Nucl. Phys. **A 738c**, 421 (2004).

[30] K. Ogata, M. Yahiro, Y. Iseri, T. Matsumoto and M. Kamimura, Phys. Rev. C **68**, 064609 (2003).

[31] A. Azhari *et al.*, Phys. Rev. Lett. **82**, 3960 (1999).

[32] A. Azhari *et al.*, Phys. Rev. C **60**, 055803 (1999).

[33] Y. Iseri, M. Yahiro and M. Kamimura, Prog. Theor. Phys. Suppl. **89**, 84 (1986).

[34] D. Baye, Phys. Rev. C **62**, 065803 (2000).

[35] N. Austern, M. Yahiro and M. Kawai, Phys. Rev. Lett. **63**, 2649(1989); N. Austern, M. Kawai and M. Yahiro, Phys. Rev. C **53**, 314 (1996); R. A. D. Piyadasa, M. Kawai, M. Kamimura and M. Yahiro, Phys. Rev. C **60**, 044611(1999).

[36] M. Yahiro and M. Kamimura, Prog. Theor. Phys. **65**, 2046 (1981); **65**, 2051 (1981).

[37] T. Matsumoto *et al*., Phys. Rev. C **68**, 064607 (2003).

[38] A. M. Moro *et al*., Phys. Rev. C **65**, 011602(R) (2002).

[39] R. Y. Rasoanaivo and G. H. Rawitscher, Phy. Rev. C **39**, 1709 (1989).

[40] M. Kawai, private communication (2003).

[41] See, for example, Y. Watanabe *et al.*, Phys. Rev. C **59**, 2136 (1999).

[42] C. Angulo *et al.*, Nucl. Phys. **A716**, 211 (2003).

[43] H. Esbensen and G. F. Bertsch, Nucl. Phys. **A600**, 37 (1996).

[44] F. C. Barker, Aust. J. Phys. **33**, 177 (1980).

[45] A. J. Koning and J. P. Delaroche, Nucl. Phys. **A713**, 231 (2003).

[46] J. Cook, Nucl. Phys. **A388**, 153 (1982).

[47] T. Motobayashi, private communication (2004).

[48] K. H. Kim, M. H. Park and B. T. Kim, Phys. Rev. C **35**, 363 (1987).

[49] I. Tanihata *et al.*, Phys. Rev. Lett. **55**, 2676 (1985).

[50] T. Matsumoto *et al*., Phys. Rev. C **70**, 061601(R) (2004).